

Synthesis, Characterization, DNA binding and cleavage, BSA interaction and Anticancer Activity of dinuclear Zinc complexes

Chun-Yan Gao^a, Xin Qiao^b, Zhong-Ying Ma^b, Zhi-Gang Wang^a, Jing Lu^a, Jin-Lei Tian^{a*},
Jing-Yuan Xu^b, Guang-Jun Xu^c, Zhi-Ling Wang^c and Shi-Ping Yan^{a*}

^a Department of Chemistry, Nankai University, Tianjin 300071, P. R. China

^b College of Pharmacy, Tianjin Medical University, Tianjin 300070, P. R. China

^c Forth Mil Med Univ, Bethune Mil Med Coll, Shijiazhuang, 050081, P. R. China

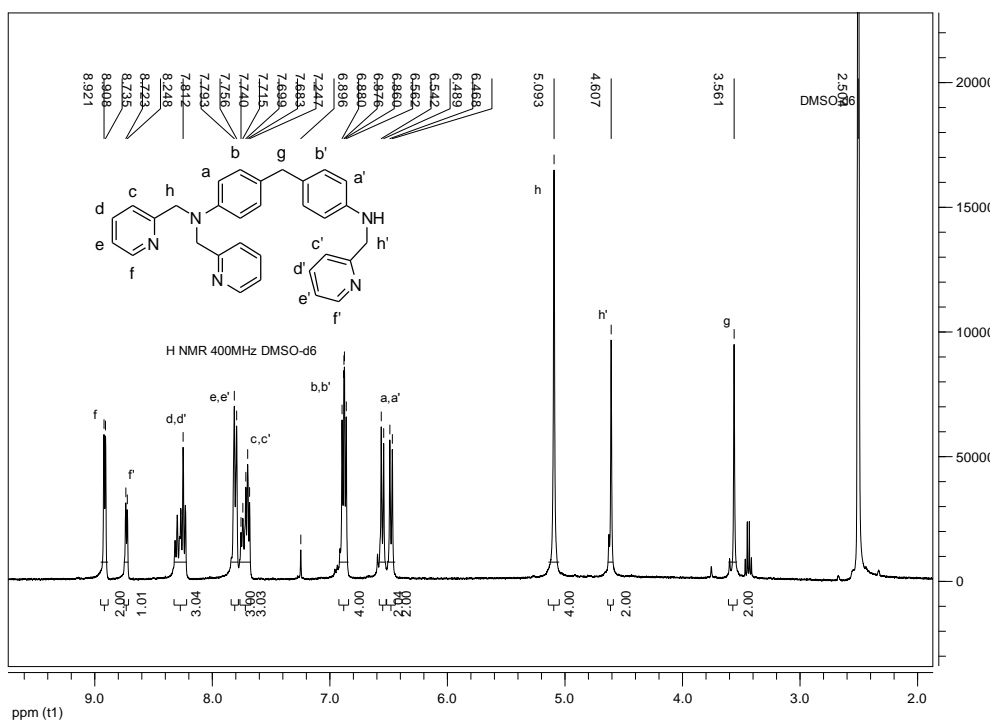


Fig. S1. ¹H NMR (400 MHz) spectra of the ligand L¹ in DMSO-d₆.

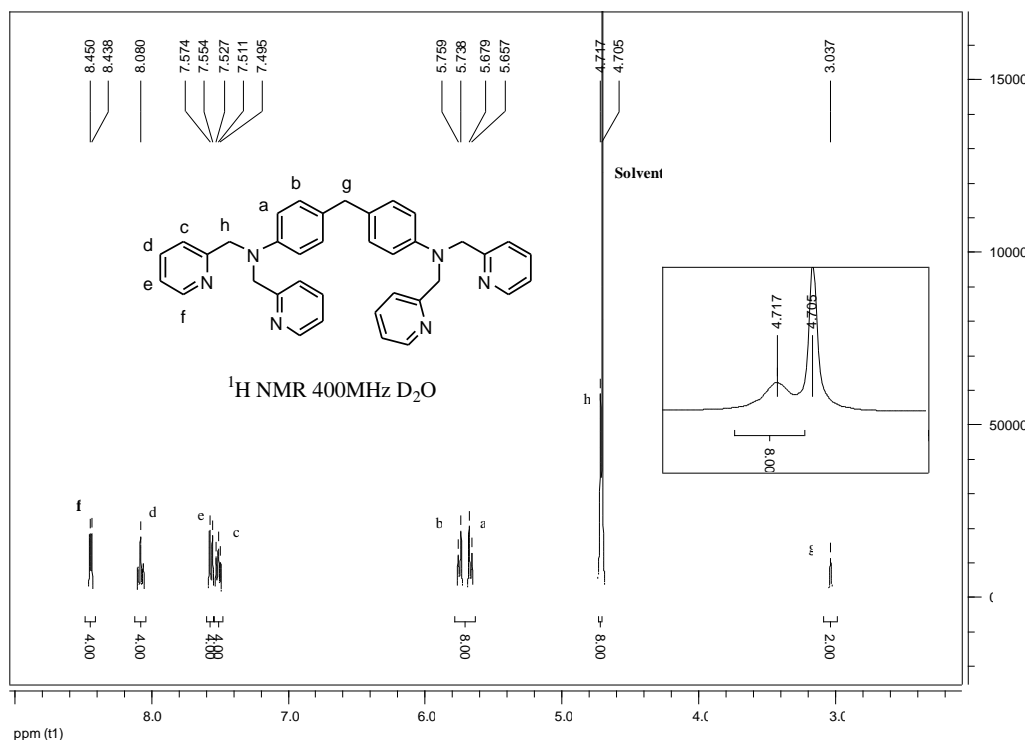


Fig. S2. ^1H NMR (400 MHz) spectra of the ligand L^2 in D_2O .

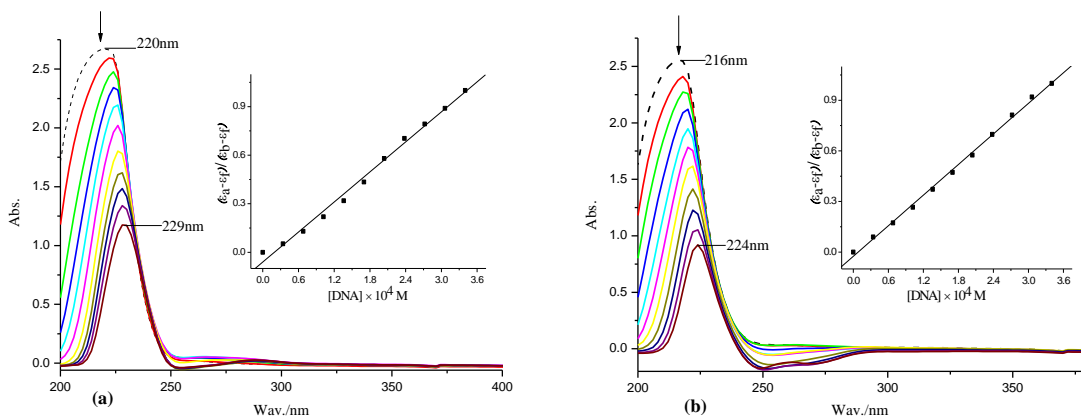


Fig. S3 (a-b) Absorption spectra of complexes **1** and **3** ($1.96 \times 10^{-6}\text{M}$) in the absence (dashed line) and presence (solid line) of increasing amounts of CT-DNA (34, 68, 102, 136, 170, 204, 238, 272, 306, and 340 μM) in 5 mM Tris-HCl/50 mM NaCl buffer (pH = 7.2). The arrow shows the absorbance changes on increasing DNA concentration. Inset: Plot of $(\epsilon_a - \epsilon_f)/(\epsilon_b - \epsilon_f)$ versus [DNA] for the titration of DNA to complex.

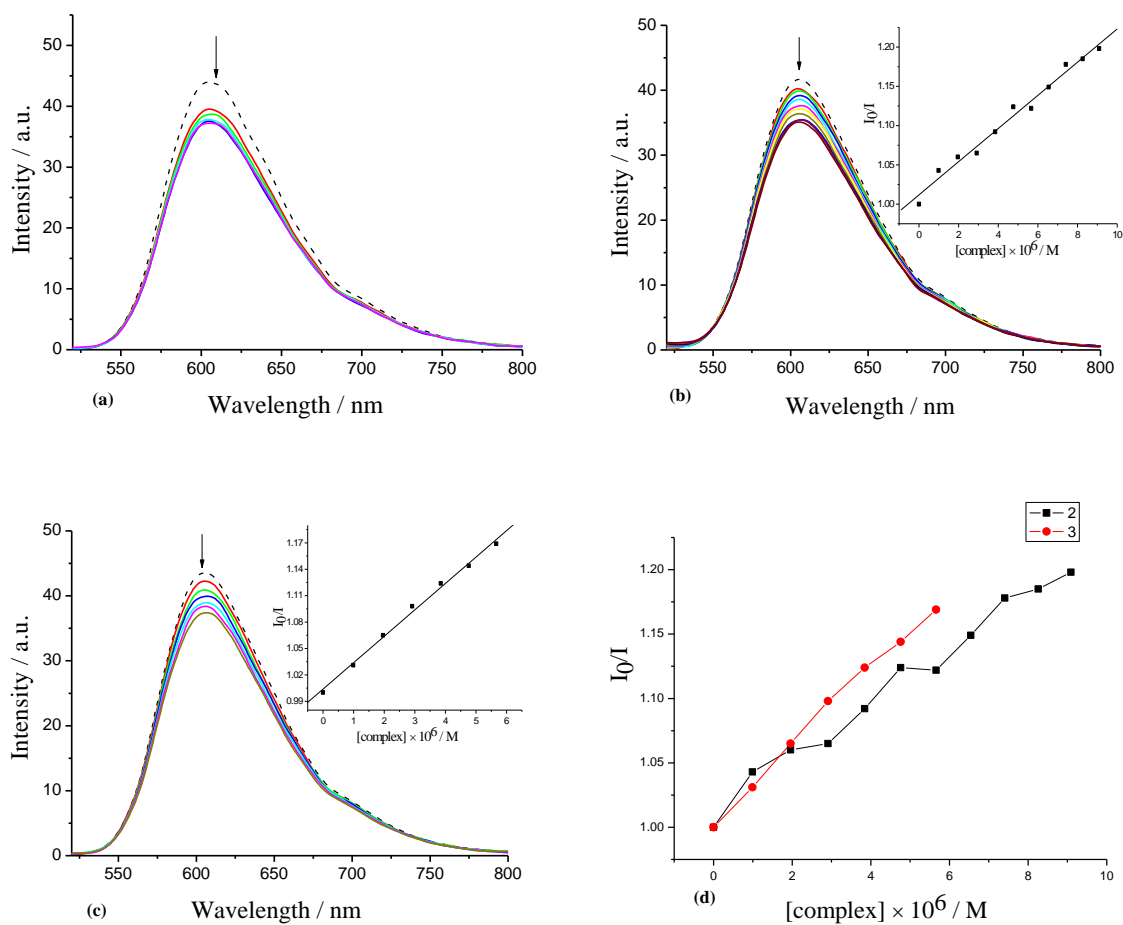
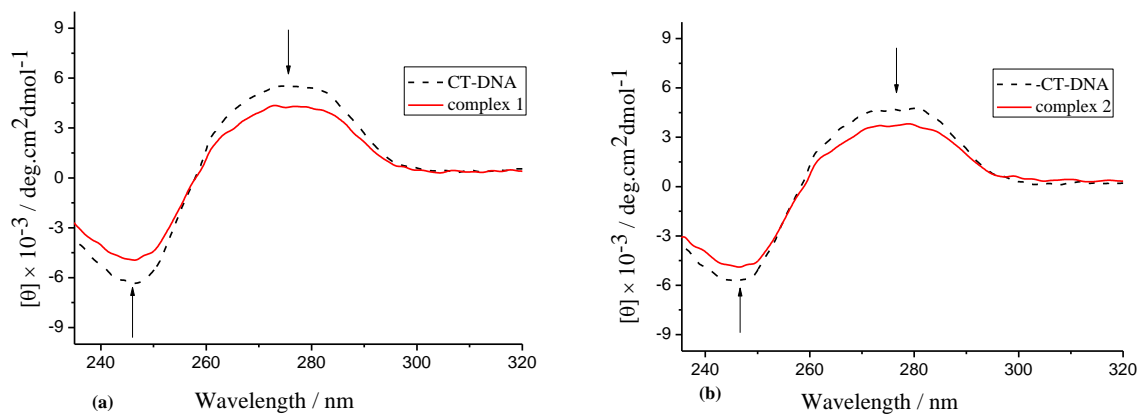


Fig. S4(a-c) Fluorescence emission spectra of the EB (2.4 μM) bound to CT-DNA (48 μM) system in the absence (dashed line) and presence (solid lines) of complexes **1-3** (0.99, 1.96, 2.91, 3.85, 4.76, 5.66, 6.54, 7.41, 8.26 and 9.09 μM). Inset: the plot of I_0/I versus the complex concentration. **(d)** The plot of I_0/I versus the concentration of complexes **2** and **3**.



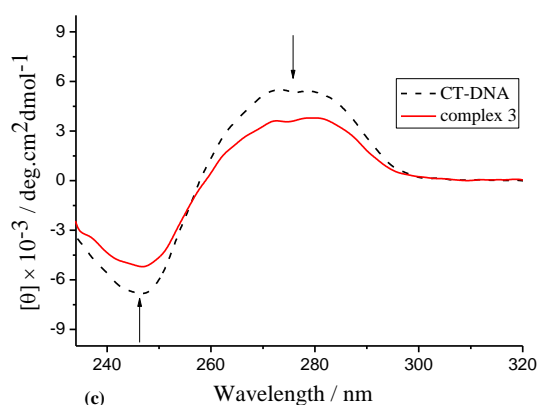


Fig. S5 (a-c) CD spectra of CT-DNA in the buffer solution (Tris-HCl) at 0.66 mM in the absence (dashed line) and presence (solid line) of 0.032 mM complex 1-3.

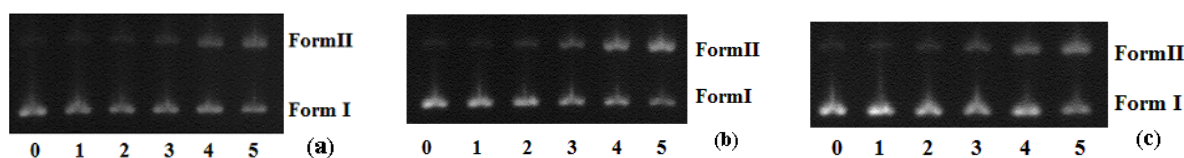


Fig. S6 (a-c) Gel electrophoresis diagram showing the cleavage of pBR322 DNA (0.1 $\mu\text{g}/\mu\text{L}$) for complexes **1-3** at different concentrations in Tris-HCl/NaCl buffer (pH = 7.2) and 37 °C. Lane 0: DNA control (4 h); Lane 1-5: DNA + **complex** (0.005, 0.025, 0.045, 0.065, 0.080 mM), respectively.

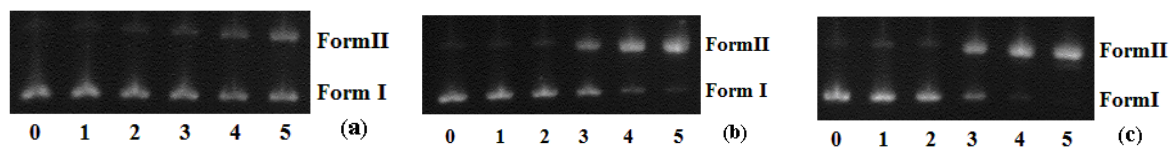


Fig. S7 (a-c) Gel electrophoresis diagrams showing the cleavage of pBR322 DNA (0.1 $\mu\text{g}/\mu\text{L}$) for **complexes 1-3** at different concentrations in Tris-HCl/NaCl buffer (pH = 7.2) and 37 °C. Lane 0: DNA control (4 h); Lane 1: DNA + 0.25 mM H_2O_2 ; Lane 2-5: DNA + H_2O_2 + **complex** (0.005, 0.025, 0.045, 0.065 mM), respectively.

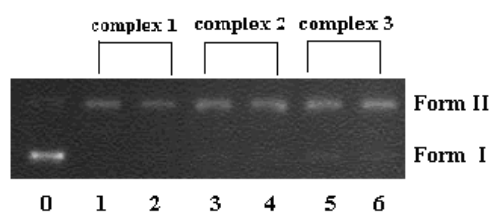


Fig. S8 Cleavage of plasmid pBR322 DNA (0.1 $\mu\text{g}/\mu\text{L}$) in presence of 0.065 mM complexes **1-3** and 20 U/mL Catalase inhibitors after 4 h incubation at 37 °C. Lane 0: DNA control; Lane 1: DNA + 0.25 mM H_2O_2 + **complex 1**; Lane 2: DNA + 0.25 mM H_2O_2 + **complex 1** + Catalase; Lane 3-4 corresponds to **complex 2**. Lane 5-6 corresponds to **complex 3**

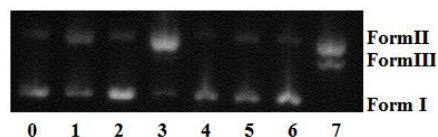


Fig. S9 Cleavage of pBR322 DNA (0.1 $\mu\text{g}/\mu\text{L}$) by complex **3** incubated for 4 h at pH 7.2 and 33 $^{\circ}\text{C}$. Lane 0-3 (in N_2 atmosphere): DNA control; DNA + 0.075 mM complex; DNA + 0.25 mM H_2O_2 ; DNA + 0.25 mM H_2O_2 + 0.075 mM complex; (Lanes 4-7 aerobic conditions).

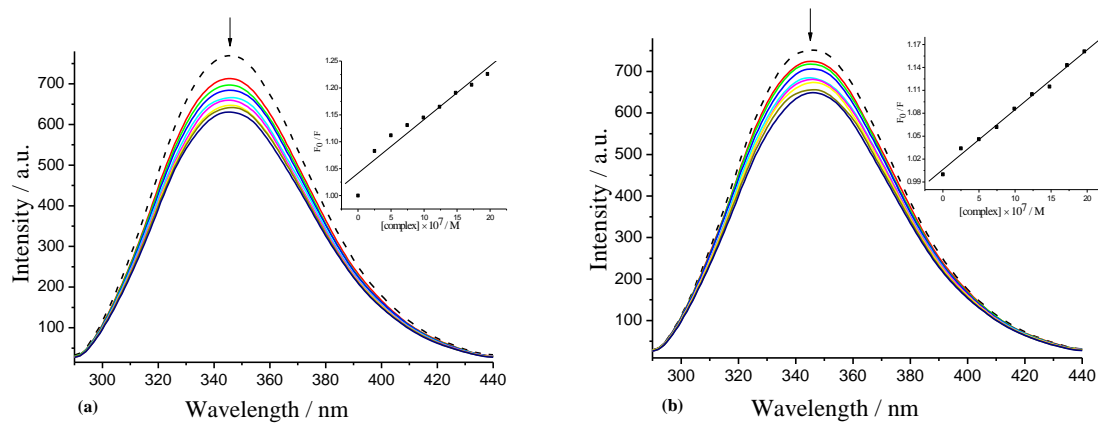


Fig. S10(a-b) Fluorescence emission spectra of the BSA (29.4 μM) system in the absence (dashed line) and presence (solid lines) of complexes **1** and **3** (0.25, 0.5, 0.74, 0.99, 1.23, 1.48, 1.72, and 1.96 μM , respectively). Inset: the plot of F_0/F versus the complex concentration.

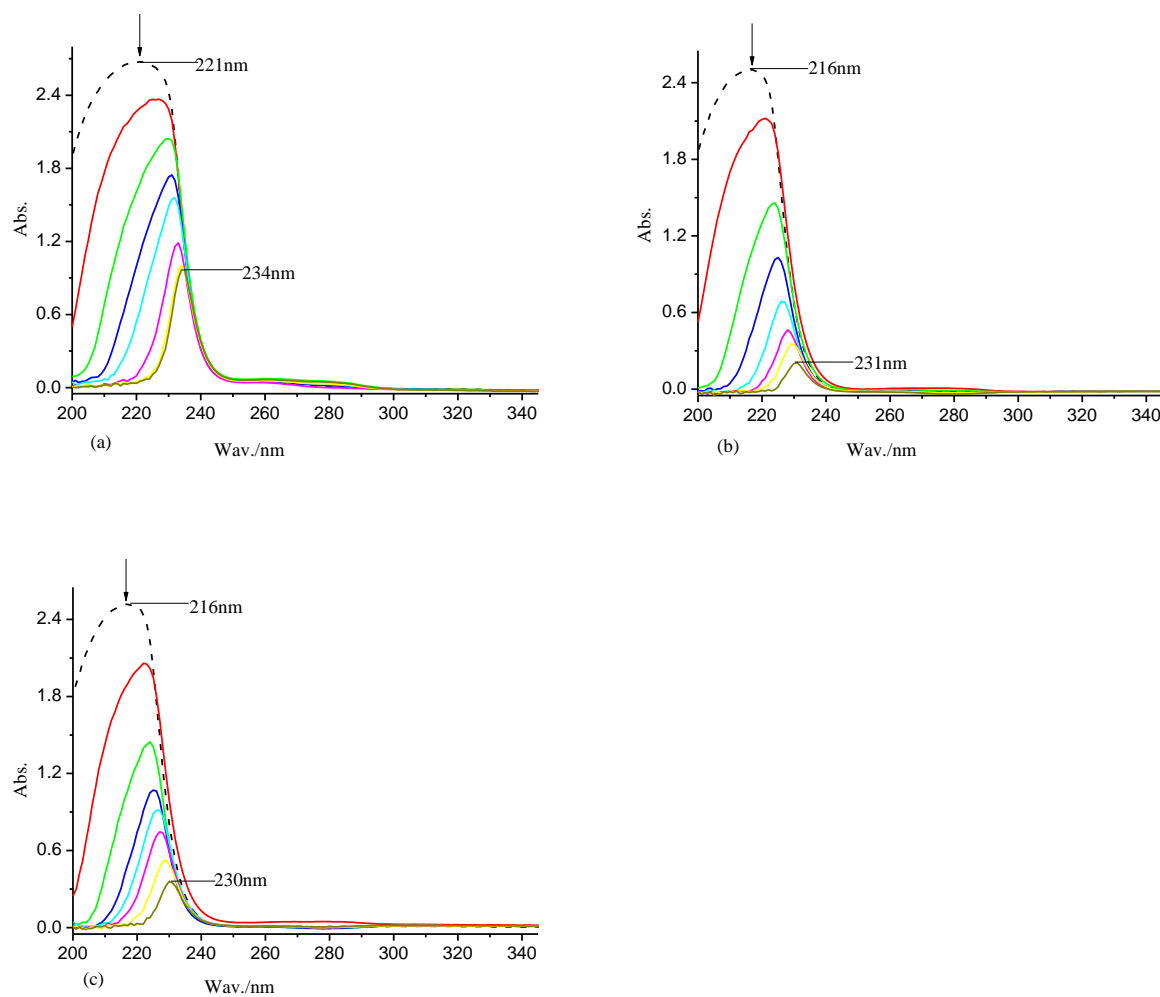


Fig. S11 (a-c) Absorption spectra of complexes **1-3** (1.96 μM) in the absence (dashed line) and presence (solid line) of increasing amounts of BSA (0.59, 1.18, 1.76, 2.35, 2.94, 3.53 and 4.12 μM) in phosphate buffer (pH = 7.0).